

# Activity–acidity relationship in zeolite Y

## Part 2. Determination of the acid strength distribution by temperature programmed desorption of ammonia

C. Costa, J.M. Lopes, F. Lemos<sup>\*</sup>, F. Ramôa Ribeiro

*Centro de Engenharia Biológica e Química, Instituto Superior Técnico, Av. Rovisco Pais 1096 Lisboa Codex, Portugal*

Received 13 June 1998; accepted 13 October 1998

### Abstract

In this paper we will have a detailed look at a numerical procedure that allows the estimation of the acid site strength distribution using a single temperature programmed desorption (TPD) experiment. The possibility of estimating these parameters is of paramount importance in the determination of quantitative relationships between activity and acidity. The application of the procedure to a set of simulated thermograms gives a clear view of the applicability of this method. The procedure was tested both in single and multi energy distributions, as well as quasi-continuum distributions. Then the method has been applied on TPD thermograms obtained from catalysts based on two different forms of zeolite Y. In part 3 of this series, the acid site distributions obtained here will be used in an activity–acidity relationship, using a Brønsted type equation, similar to the one used in homogeneous acid catalysis. © 1999 Elsevier Science B.V. All rights reserved.

*Keywords:* Zeolites; Y zeolite; Acidity; TPD

### 1. Introduction

Zeolites are widely used catalysts for reactions involving acid catalysts. Their main application, in catalytic cracking, corresponds to the process that consumes the largest amounts of solid catalysts.

The relation between acidity and activity has been long sought for catalytic cracking. However, unlike the case of homogeneous acid-catalysed reactions, for which there are known relations between the acid strength of the catalyst and reaction rates (the Brønsted relations),

this has not yet been achieved for heterogeneous catalysed reactions. Two main difficulties have hindered progress in this area: (i) the solid catalysts cannot be represented by a single acid strength. They present a quasi-continuous distribution of acid strengths, corresponding to acid sites with different environments; (ii) the determination of acid strength distribution is not simple and poses severe difficulties at both experimental and interpretation levels.

A good deal of attention has been paid to temperature programmed desorption of ammonia, or other bases, as a relatively efficient method of determining total acid strength, as well as acid strength distributions, at least at a

<sup>\*</sup> Corresponding author

comparative level. Some review papers about this technique and its application in catalytic systems have been published in recent years [1–6].

Temperature programmed desorption of bases can very easily show differences in the acidity between catalysts. Nevertheless, some difficulties are encountered when trying to quantify these differences because the peaks due to desorption from acid sites with different strength overlap extensively, leading to complex thermograms.

The classical usage of TPD involves a succession of experiments that are lengthy to carry out and give only a rather limited amount of information regarding the acid strength of the solid [7–9]. However, several methods have been proposed to allow the use of a single TPD experiment to obtain more detailed information concerning the acid strength distribution of a zeolite [10–17].

We have already presented a preliminary report on a method to obtain acid strength distributions, based on a numerical deconvolution of a single TPD experiment [18]. We will now give a detailed examination of how it works and how the information gathered can be used to correlate acidity and catalytic cracking activity in a set of ion-exchanged Y zeolites.

In the following pages, we will start by presenting a brief description of the theoretical background, followed by validation of the deconvolution method on simulated thermograms and then application of the method to TPD thermograms obtained from some zeolite catalysts.

## 2. Theory

In order to obtain the strength distribution of the acid sites, on the catalyst surface, as a function of the activation energy for ammonia desorption, a numerical procedure to perform the digital deconvolution of the TPD curves, experimentally obtained, into the uniform en-

ergy components was developed. The area under each of these mono-energetic curves is proportional to the relative amount of acid sites with that energy.

The method was developed with the assumption that no interaction between the adsorbed molecules occurs, that desorption is irreversible (i.e., no readsorption takes place) and presents a first order kinetics. We have also assumed that each type of acid sites is characterised by a particular value of the kinetic rate constant for the desorption of the base, expressed by an Arrhenius-type expression and that the pre-exponential factor is a simple function of the activation energy.

Since the experiments are carried out in a flow cell, thus keeping the partial pressure of the adsorbate at very low levels at all the time, we take these approaches as good. The same considerations have been made by other authors proposing related techniques [12–15] and are usually taken to be reasonable approximations.

Using the above mentioned assumptions, the desorption from a set of sites with uniform energy,  $E$ , can be described by kinetic Eq. (1).

$$-\frac{dq_E}{dt} = k_E e^{-E/RT} q_E \quad (1)$$

where  $q_E$  is the amount of molecules adsorbed in sites with energy  $E$  and  $k_E$  is the pre-exponential factor for the kinetic rate constant.

To obtain the variation of  $q_E$  with time, one has to integrate Eq. (1), taking into consideration that the temperature varies linearly with time ( $T = T_0 + v_T t$ ) and that at time zero the amount of sites with energy  $E$  occupied with ammonia is  $q_{E0}$ . This integration leads to Eq. (2).

$$\ln\left(\frac{q_E}{q_{E0}}\right) = -\int_{T_0}^T \frac{k_E}{v_T} e^{-E/RT} dT \quad (2)$$

Substituting Eq. (2) in Eq. (1), we obtain the rate of desorption from this type of site:

$$-\frac{dq_E}{dt} = k_E q_{E0} e^{-E/RT - \int_{T_0}^T \frac{k_E}{v_T} e^{-E/RT} dT} \quad (3)$$

Since the catalyst has sites with widely different energies, in order to obtain the total amount of base desorbed, we will have to perform the summation of the contributions from all the possible energies.

Thus, if we consider a finite set of energies, which we will represent by  $E^i$ , we will obtain Eq. (4).

$$-\frac{dq}{dt} = \sum_i k_{E^i} e^{-E^i/RT} q_{E^i} \quad (4)$$

where  $q_{E^i}$  is the amount of molecules adsorbed in acid sites presenting an activation energy for the desorption of ammonia of  $E^i$  and  $k_{E^i}$  is the corresponding pre-exponential factor.

Although it is possible that the strength distribution of the acid sites would be better described by a continuous probability density function, this is not a major problem if one considers that each individual energy value represents, in fact, an interval and that the  $q_{E^i}$  values that are obtained, represent the amount of acid sites with desorption energies within that range.

By fitting experimental data to Eq. (4) it is possible to determine the values of  $q_{E^i}$  for a particular catalyst, as long as the values of  $k_E$  are known as a function of  $E$ .

According to Hashimoto et al. [12] the relation between the pre-exponential rate constant and the activation energy can be expressed by:

$$k_E = \alpha e^{\beta E} \quad (5)$$

where  $\alpha$  and  $\beta$  are positive constants. This relation is similar to the Brønsted equation, relating the kinetic constant for a particular acid catalysed reaction with the acidity of the catalyst and, as we will try to, can be adequately applied to desorption of ammonia in zeolite Y. The values of  $\alpha$  and  $\beta$  were estimated experimentally as shown in Section 4.

Thus, the right hand of Eq. (4) will be the weighted summation of the curves generated by integration of Eq. (3) for each of the energy

values in the set considered and the left hand represents the observed flux of ammonia desorbed, which is obtained experimentally.

The decomposition procedure will then, imply the choice of an energy set, the computation of Eq. (3) for all the energies in this set, and the estimation of the values of the  $q_{E^i}$  values that better describe each experimental TPD curve.

Despite the fact that this involves, in fact, a very large number of computations, the power needed to perform this decomposition procedure is now available even on a medium range IBM compatible personal computer, using a commercial spreadsheet program, thus rendering this method easily accessible to the experimental researcher at the laboratory bench.

Moreover, the use of Eq. (4) in this way, can also take into account possible incorrections in the temperature change with time. In fact, most of the experiments of this type will show, at one time or another, deviations from the linear increase in temperature that is usually assumed in the processing of TPD data. However, if the integration of Eq. (4) is done using the actual temperature profile of an experiment, this source of error will be eliminated from the procedure.

### 2.1. Decomposition procedure

The procedure just described can be outlined in the following sequence of steps.

(i) Choice of the energy set. This choice should be mainly conditioned by the precision one wishes to have in the final distribution as well as the amount of computation required and the possible increase in numerical error if the separation of the energies is too small. This effect is due to the extensive overlap between individual desorption curves in these conditions. The larger the energy set the more precise will the distribution be but longer the computations will take. The energy set that will be generally used in this paper is the following (energy values in kJ/mol): 45, 50, 55, 60, 65, 70, 75, 80, 90, 100, 120, 140, 180, 200.

(ii) Computation of  $k_{E^i}$  values for all the energies chosen, using Eq. (5). The values of the  $\alpha$  and  $\beta$  parameters can be obtained experimentally for a particular catalyst and then applied to a whole series of related ones, as described by Hashimoto et al. [12].

(iii) Solution of Eq. (3) for all the energies in the set, using the actual temperature profile of the experiment under analysis and considering  $q_{E0^i} = 1$ . In fact, Eq. (4) can be re-written as

$$-\frac{dq}{dt} = \sum_i k_{E^i} e^{-E^i/RT} q_{E^i} \\ = \sum_i q_{E0^i} \left( k_{E^i} e^{-E^i/RT} - \int_{t_0}^t k_{E^i} e^{-E^i/RT} dt \right) \quad (6)$$

in which the curves represented by the term under brackets on the right-hand side correspond the single energy desorption curves with unity initial amount of sites. This can be done due to the assumption that desorption is irreversible and that there are no interactions between different sites.

(iv) Determination of  $q_{E0^i}$  values by multi-linear least-square regression fitting of the experimental thermogram with the weighted sum of the theoretical curves obtained in the previous step, either using a dedicated program or a commercial spreadsheet. The computations presented in this paper were performed in Excel 5 (© Microsoft) using the solver tool to minimise the sum of the square of the residuals by varying the values of  $q_{E0^i}$ .

## 2.2. Application of digital deconvolution method on simulated thermograms

In order to verify the applicability of the deconvolution method developed, the procedure was tested both in single and multi energy distributions (as well as quasi-continuous ones) generated using Eq. (3).

The following situations were simulated: (i) two thermograms with unimodal energy distri-

bution with  $E = 60$  and  $90$  kJ/mol, respectively; (ii) one thermogram with bimodal energy distribution with  $E = 60$  and  $90$  kJ/mol; (iii) two thermograms whose energy distribution is described by gaussian functions around the medium values of energy of  $60$  or  $90$  kJ/mol, respectively; (iv) one thermogram whose energy distribution is described by the superposition of two gaussian distributions, one around  $60$  kJ/mol and the other one around  $90$  kJ/mol.

In Fig. 1, as an example, this last situation is shown as well as the components curves obtained using the deconvolution method explained above. The application of this method in which only a finite number of acid strengths has been considered leads to excellent fittings, even on thermograms which have been obtained using a quasi-continuous distribution of energies.

Not only the fitting to the actual thermogram is quite good, but also the acid strength distribution have an excellent agreement with the one that was actually used in generating the curves. In Fig. 2 the cumulative acid site distribution against activation energy and the values estimated by application of the deconvolution method, are plotted for the same example shown

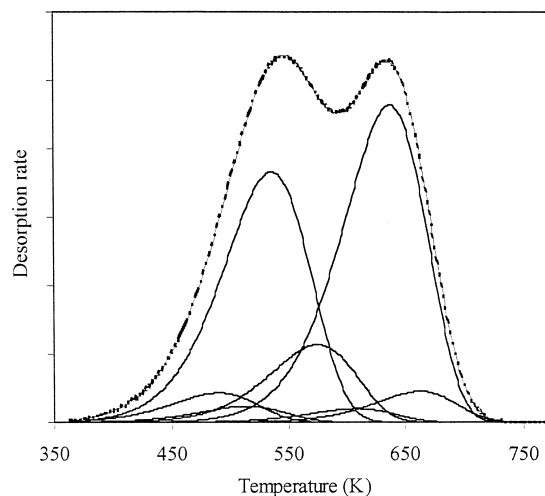


Fig. 1. Simulated thermogram (—) generated by the superposition of two gaussian distributions, one around  $60$  kJ/mol and the other one around  $90$  kJ/mol. Fitting (---) and component curves obtained by application of deconvolution method.

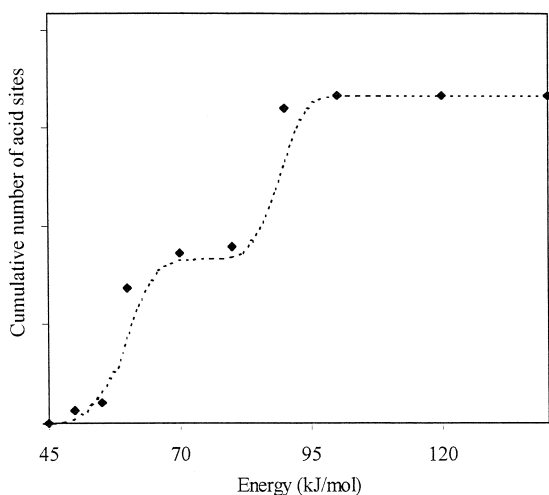


Fig. 2. Cumulative acid site distribution against the energies values of the simulated thermogram generated by the superposition of two gaussian distributions, one around 60 kJ/mol and the other one around 90 kJ/mol (---) and the values estimated by application of deconvolution method (◆).

in Fig. 1. The application of the procedure to this set of simulated thermograms allowed us to conclude that using a discrete basis of energies instead of a continuous one does not correspond

to a serious limitation and does, in fact, describe the data in a very reasonable manner.

### 3. Experimental

#### 3.1. Catalysts

In order to have catalysts with a wide range of acidity, two series of catalysts, based on two different forms of zeolite Y, were prepared. The HNaY series of catalysts was obtained from a NaY zeolite (LZ-Y52, Union Carbide) by successive ion-exchange with  $\text{NH}_4\text{NO}_3$  solutions, and the HNaUSY series from an  $\text{NH}_4\text{USY}$  zeolite (LZ-Y82, Union Carbide) by successive ion-exchange with  $\text{NaNO}_3$  solutions.

Details of the preparations have been given in part 1 [19] of this paper.

#### 3.2. Apparatus and procedure

The TPD measurements were carried out in an apparatus which is schematically represented by Fig. 3. About 200 mg of zeolites samples

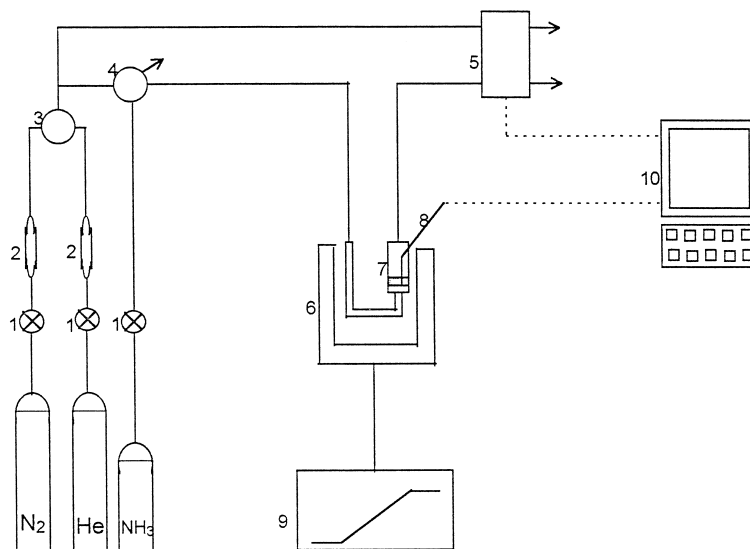


Fig. 3. Scheme of the apparatus for temperature-programmed desorption: 1, regulation valves; 2, dryers (molecular sieves 13X-BDH); 3, six-way valve; 4, dosing valve; 5, thermal conductivity detector (inside a gaseous chromatographic Shimadzu GC-9A); 6, oven; 7, U-shaped cell where the catalyst sample is placed; 8, thermocouple; 9, temperature programmer and PID controller (Shimaden FP21); 10, personal computer. The lines where ammonia and helium went through were heated, at 120°C, to avoid the physical adsorption of ammonia.

were put in a quartz cell with U shape and pretreated, in situ, during 12 h at 450°C in a flow of nitrogen (> 99%) of 60 ml/min. After cooling to 90°C, adsorption of ammonia (> 99.995%) was carried out in a flow of dry helium (> 99%) of 60 ml/min. After the catalyst surface became saturated some time was waited to remove the excess of ammonia. The temperature-programmed desorption was carried out with a linear heating rate of approximately 7.5°C/min from 90°C to 700°C. The NH<sub>3</sub> that desorbed was measured by a thermal conductivity detector and the electrical signals from the detector and from the thermocouple (that measures the temperature inside the cell with the catalyst) were digitised by a CR3A chromatographic integrator and transmitted to a computer.

To examine the reproducibility of the data, several samples of the same zeolite were tested more than once. It was found that the reproducibility of the experiments is good.

## 4. Results and discussion

### 4.1. Blank experiments

Some blank experiments were carried out under the experimental conditions previously described but in absence of zeolite—‘blanks without catalyst’—in order to verify if the ammonia retained in the lines was significant. As the detector signal during these experiments did not increase, one can conclude that the amount of ammonia retained by the system itself is negligible.

Some TPD experiments were also carried out, under the same experimental conditions, over the catalyst but without ammonia admission—‘blanks with catalyst’—in order to verify if other processes (namely dehydroxylation) took place [14,20–22]. A typical example of a TPD thermogram of NH<sub>3</sub> over HNaUSY83 catalyst and the correspondent ‘blank with catalyst’, is shown in Fig. 4.

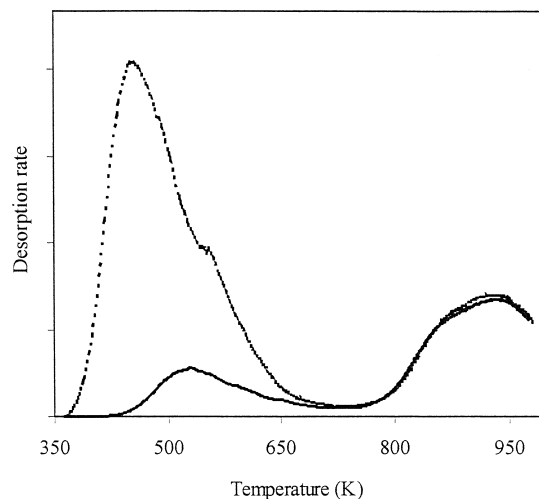


Fig. 4. TPD thermogram of NH<sub>3</sub> from HNaUSY83 catalyst (---) and the corresponding blank experiment, done over the same catalyst and under the same experimental conditions but without NH<sub>3</sub> admission (—).

A desorption peak for temperatures above 750 K is observed, but neither its intensity nor the temperature of its maximum follow a regular trend with protonic content of zeolite. This peak was attributed to the dehydroxylation of the catalyst, because it was observed in the corresponding ‘blanks with catalyst’.

In computations to obtain the deconvolution of TPD thermograms these were base-line corrected using the corresponding ‘blank with catalyst’.

### 4.2. Estimation of $\alpha$ and $\beta$ values of $k_E(E)$

As explained above Eq. (5) is used to describe the relation between  $k_E$  and  $E$ . A series of TPD thermograms for the acid sites with uniform acid strength is required to determine the  $\alpha$  and  $\beta$  constants [12]. Thus, a set of TPD experiments over HNaY40 and USHY catalysts (Figs. 5 and 6, respectively) were carried out by raising the ammonia adsorption temperature ( $T_0$ ) by a small amount,  $\Delta T$ .

When the increment in temperature is sufficiently small, the difference curve between two consecutive desorption thermograms represents

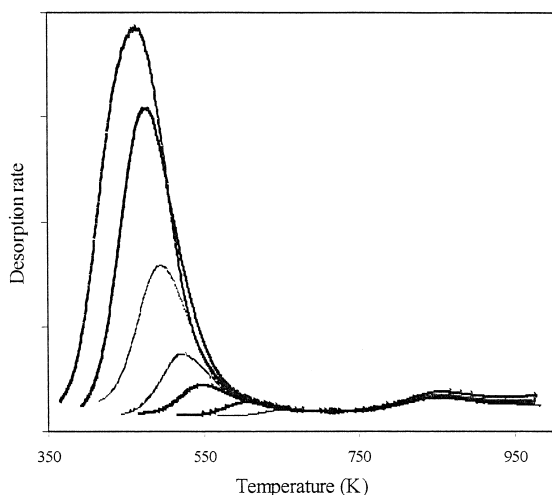


Fig. 5. TPD thermograms of  $\text{NH}_3$  carried out over HNaY40 zeolite with the following adsorption temperatures (K): 363, 388, 413, 438, 463, 513, 563.

the desorption thermogram of ammonia from acid sites with uniform acid strength. Each of these curves is then fitted to Eq. (1) and  $k_E$ ,  $q_{E0}$  and  $E$  values were estimated by non-linear regression.

The TPD thermograms of  $\text{NH}_3$  from acid sites having uniform acid strength, performed over HNaY40 and USHY zeolites and the correspondent fittings are shown in Figs. 7 and 8,

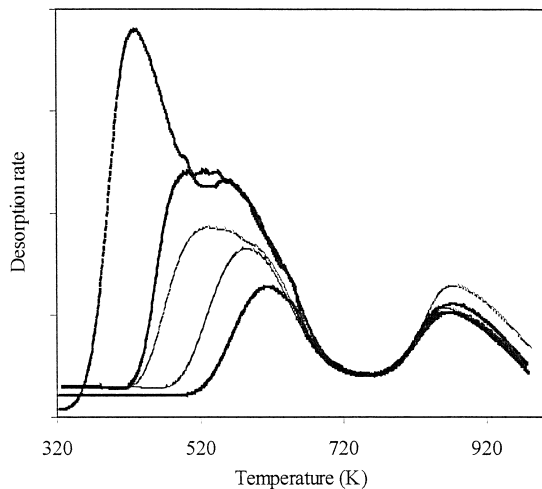


Fig. 6. TPD thermograms of  $\text{NH}_3$  carried out over USHY zeolite with the following adsorption temperatures (K): 363, 413, 463, 513, 563.

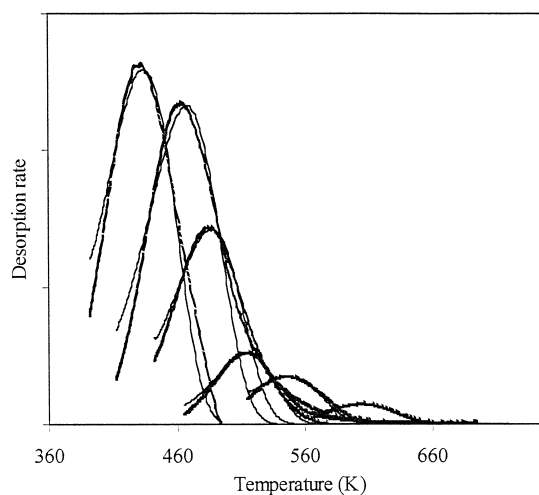


Fig. 7. TPD thermograms of  $\text{NH}_3$  from acid sites having uniform acid strength (obtained subtracting thermograms performed with different ammonia adsorption temperature) carried out over HNaY40 zeolite. Lines are obtained by fitting the experimental data with Eq. (1).

respectively. The results obtained by the fittings are collected in Table 1. The quality of the fitting indicates that a mono-strength TPD curve is, indeed, a good description for the TPD-difference curves described above.

In Fig. 9 the logarithm of  $k_E$  is plotted against  $E$  using the values from Table 1. These

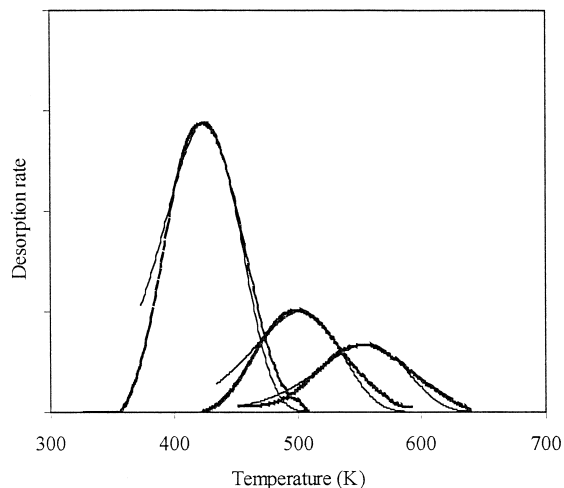


Fig. 8. TPD thermograms of  $\text{NH}_3$  from acid sites having uniform acid strength (obtained subtracting thermograms performed with different ammonia adsorption temperature) carried out over USHY zeolite. Lines are obtained by fitting the experimental data with Eq. (1).

Table 1

$E$  and  $k_E$  values estimated by fitting Eq. (1) to the TPD thermograms of  $\text{NH}_3$  from acid sites having uniform acid strength (see text for details)

$T_0$ (K)	$T_0 + \Delta T$ (K)	$E$ (KJ/mol)	$k_E$ ( $\text{s}^{-1}$ )
<i>HNaY40</i>			
363	388	55.3	$2.2 \times 10^4$
388	413	60.8	$2.8 \times 10^4$
413	438	68.2	$9.8 \times 10^4$
438	463	87.5	$4.0 \times 10^6$
463	513	84.1	$4.9 \times 10^5$
513	563	100.2	$2.0 \times 10^6$
<i>USHY</i>			
363	413	44.0	$9.8 \times 10^2$
463	513	54.4	$1.6 \times 10^3$
513	563	66.1	$5.7 \times 10^3$

values are well described by the following relation, indicating that Eq. (5) is held for desorption of ammonia from acid sites:

$$k_E = 1.45e^{0.15E} \quad (7)$$

The computation procedure used to estimate the  $k_E$  values as a function of  $E$  has some advantages relatively to the one proposed by Hashimoto et al. [12] (some of them had already been mentioned in Ref. [13]) since it does not consider only the experimental datum corresponding to the maximum temperature of TPD

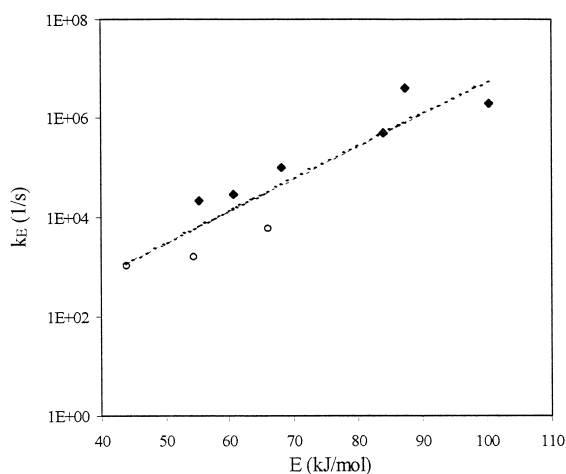


Fig. 9. Dependency of frequency factor,  $k_E$ , on the activation energy for the ammonia desorption on (◆) HNaY40 and (○) USHY, zeolites.

curve but makes use of the whole set of experimental data and a non-linear least square method is used to determine simultaneously the values of  $E$  and  $k_E$ , giving good fittings to the experimental data and a better support to the values that were computed.

### 4.3. Characterisation of catalysts acidity

In order to evaluate the catalyst acidity, TPD of  $\text{NH}_3$  experiments were performed over all catalysts and subsequently the deconvolution method, explained above, was applied.

In Fig. 10 some TPD of  $\text{NH}_3$  thermograms, after the correspondents 'blanks with catalyst' had been subtracted, are plotted depicting the wide range of acidity that was covered with these series of catalysts.

$\text{NH}_3$  is a polar molecule with permanent electric dipole moment of  $\mu = 1.30$  D [23]. There is some interaction between  $\text{NH}_3$  molecules and  $\text{Na}^+$  cations when these cations are present in zeolites [24,25]. Thus, the amount of  $\text{NH}_3$  retained in Na forms of zeolites is not negligible, and can be of the same order of magnitude of the amount of  $\text{NH}_3$  adsorbed on other catalysts with different ion-exchange lev-

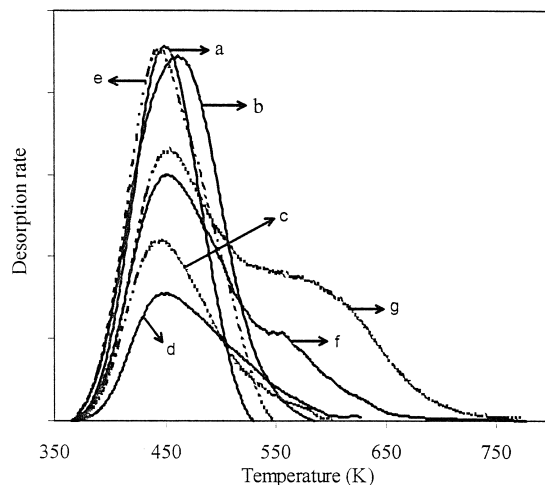


Fig. 10. TPD of  $\text{NH}_3$  thermograms from (a) NaY; (b) HNaY40; (c) HNaY80; (d) HNaY91; (e) HNaUSY3; (f) HNaUSY83; (g) USHY. Values corrected by subtracting the corresponding 'blank with catalyst' data.



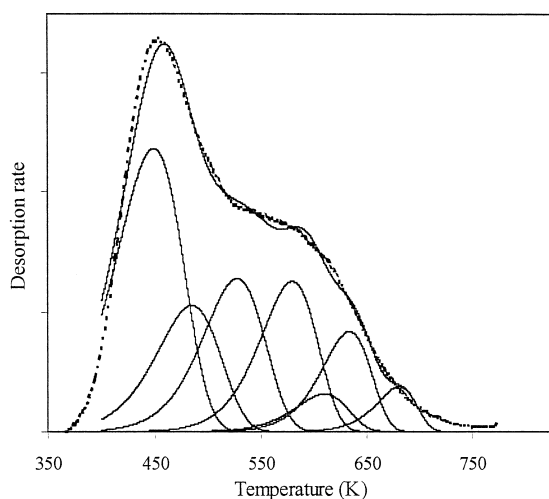


Fig. 11. TPD of  $\text{NH}_3$  thermogram carried out over USHY catalyst. Lines are the fitting and the component curves obtained by the application of the deconvolution method.

els [26]. Nevertheless, this interaction is not so strong as the interaction between  $\text{NH}_3$  molecules and protonic sites and thus the corresponding peak appears for lower values of temperature. It was verified that peak associated with this interaction is bigger when the  $\text{Na}^+$  level is higher,

as we would expect. The catalysts NaY and HNaUSY3 which have almost no protonic sites, adsorb a significant amount of ammonia and have similar thermograms.

In Fig. 11 a typical example of a thermogram, carried out over USHY catalyst, corresponding fitting and the components curves obtained after the decomposition method is shown. The area below TPD thermograms is proportional to the total sites of the catalyst where ammonia is adsorbed whereas the area below each component curve is proportional to the number of acid sites with each of the values for the activation energy for ammonia desorption. These values are collected in Table 2 for all catalysts under study. The acid site distribution, for some catalysts, is depicted in Fig. 12.

The extent of ion-exchange modifies the energy distribution of the acid sites, namely inducing an increase of strong acid sites when sodium levels decreases. Thus, for the same catalysts series, as the protons number increases, the relative number of acid sites with higher activation energy for ammonia desorption increases. This agrees with what it described in Ref. [27].

Table 2

Relative number of acid sites (%) as a function of the activation energy for ammonia desorption for all catalysts under study. Results obtained by decomposition method application on TPD of  $\text{NH}_3$  thermograms

	Relative number of acid sites (%)													
	Energy (kJ/mol)													
	45	50	55	60	65	70	75	80	90	100	120	140	180	200
<i>HNaY series</i>														
NaY	0.0	76.0	16.5	7.5	0.0	0.0	0.0	0.0	0.0	0.0	0.0	0.0	0.0	0.0
HNaY25	0.0	47.4	0.0	49.4	0.0	3.2	0.0	0.0	0.0	0.0	0.0	0.0	0.0	0.0
NaY40	0.0	52.6	0.0	4.05	0.0	0.0	0.0	7.0	0.0	0.0	0.0	0.0	0.0	0.0
HNaY56	0.0	54.3	0.0	22.3	0.0	19.6	0.0	0.0	0.0	3.8	0.0	0.0	0.0	0.0
HNaY73	4.1	44.9	22.2	0.0	0.0	21.6	0.0	1.7	0.0	5.5	0.0	0.0	0.0	0.0
HNaY80	39.4	0.0	43.4	4.6	0.0	0.0	0.0	12.5	0.0	0.0	0.0	0.0	0.0	0.0
HNaY85.5	6.5	47.1	0.0	26.5	0.0	15.6	0.0	0.0	3.3	1.1	0.0	0.0	0.0	0.0
NaY91	0.0	52.6	0.0	14.5	0.0	22.5	0.0	0.0	8.8	0.0	0.0	1.7	0.0	0.0
<i>HNaUSY series</i>														
HNaUSY3	19.9	55.4	0.0	0.0	24.6	0.0	0.0	0.0	0.0	0.0	0.0	0.0	0.0	0.0
HNaUSY71	32.5	0.0	44.3	0.0	0.0	16.4	0.0	6.2	0.3	0.0	0.0	0.0	0.0	0.0
HNaUSY83	3.6	42.2	0.0	23.0	0.0	6.4	0.0	11.1	0.0	9.8	0.9	3.0	0.0	0.0
HNaUSY94	0.0	36.8	0.0	13.6	0.0	11.4	0.0	9.1	6.7	8.6	6.6	4.6	2.5	0.0
USHY	0.0	34.2	0.0	15.3	0.0	0.0	17.9	0.0	0.0	16.1	3.8	9.3	0.0	3.4

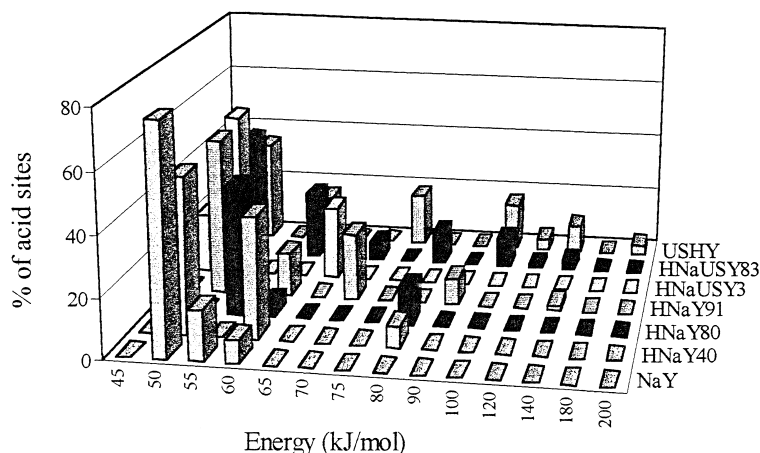


Fig. 12. Acid sites distribution (%) on relating activation energies for ammonia desorption on some HNaY and HNaUSY catalysts.

The catalysts of the HNaUSY series have sites with activation energy for the desorption of ammonia much higher than the catalysts of HNaY series. In fact, while in the most acidic catalyst of HNaY series—HNaY91—the higher value of activation energy for ammonia desorption is 140 kJ/mol, in the most acidic catalyst of HNaUSY series—USHY—the same value is 200 kJ/mol. These results are in agreement with the higher value of Si/Al on HNaUSY catalysts and with the fact that these catalysts have extra-framework  $\text{Al}^{3+}$ , characteristics which reputedly confer a high acidity to the catalysts.

The quantitative information obtained after deconvolution method application also agrees with what is qualitatively expected by TPD thermograms analysis.

## 5. Conclusions

The main conclusion that can be drawn is that the deconvolution procedure proposed is able to interpret the complex TPD patterns that are obtained from ammonia desorption from these zeolites.

The acid site distributions that are obtained can be used to quantify the acidity of these samples and, as we will show, in the continua-

tion of this series of papers, can also be used to obtain quantitative relationships between the catalytic activity and acidity measurements.

This study also verified that the proposal made by Hashimoto et al. [12] that the kinetic rate constant for the desorption can be described as a function of the activation energy by a relation similar to the Brönsted equation holds.

## Acknowledgements

We wish to thank Junta Nacional de Investigação Científica e Tecnológica for the support given, in particular with the PhD grant PRAXISXII/BD/5793/95 for Carla Costa.

## References

- [1] S. Bhatia, J. Beltramini, D.D. Do, *Catal. Today* 7 (3) (1990) 209.
- [2] J.L. Falconer, J.A. Schwarz, *Catal. Rev. Sci. Eng.* 24 (1983) 141.
- [3] R.L. Gorte, *J. Catal.* 75 (1982) 164.
- [4] R.A. Demmin, R.J. Gorte, *J. Catal.* 90 (1984) 32.
- [5] Y.-J. Huang, J.A. Schwarz, *J. Catal.* 99 (1986) 249.
- [6] A.V. Sklyarov, *Russ. Chem. Rev.* 55 (3) (1986) 214.
- [7] R.J. Cvetanovic, Y. Amenomiya, *Adv. Catal.* 17 (1967) 103.
- [8] R.J. Cvetanovic, Y. Amenomiya, *Catal. Rev.* 6 (1972) 21.
- [9] M. Sawa, M. Niwa, Y. Murakami, *Zeolites* 10 (1990) 307.
- [10] R.E. Richards, L.V.C. Rees, *Zeolites* 6 (1986) 17.
- [11] E. Dima, L.V.C. Rees, *Zeolites* 7 (1987) 219.

- [12] K. Hashimoto, T. Masuda, T. Mori, in: Y. Murakami, A. Lijima, J.W. Word (Eds.), *Stud. Surf. Sci. Catal.* 23 (1986) 503.
- [13] L. Forni, E. Magni, *J. Catal.* 112 (1988) 437.
- [14] L. Forni, E. Magni, E. Ortoleva, R. Monaci, V. Solinas, *J. Catal.* 112 (1988) 444.
- [15] H.G. Karge, V. Dondur, *J. Phys. Chem.* 94 (1990) 765.
- [16] H.G. Karge, V. Dondur, J. Weitkamp, *J. Phys. Chem.* 95 (1991) 283.
- [17] B. Hunger, M.V. Szombathely, J. Hoffmann, P. Brauner, *J. Therm. Anal.* 44 (1995) 293.
- [18] C. Costa, J.M. Lopes, F. Lemos, F.R. Ribeiro, *Catal. Lett.* 44 (1997) 255.
- [19] C. Costa, J.M. Lopes, F. Lemos, F.R. Ribeiro, *J. Mol. Catal. A: Chem.* 144 (1999) 207.
- [20] A. Corma, V. Fornés, F.V. Melo, J. Herrero, *Zeolites* 7 (1987) 559.
- [21] B.M. Lok, B.K. Marcus, C.L. Angell, *Zeolites* 6 (1986) 185.
- [22] C.V. Hidalgo, H. Itoh, T. Hattori, M. Niwa, Y. Murakami, *J. Catal.* 85 (1984) 362.
- [23] E. Dima, L.V.C. Rees, *Zeolites* 10 (1990) 8.
- [24] V.R. Choudhary, S.G. Pataskar, *Zeolites* 6 (1986) 307.
- [25] I.V. Mishin, A.V. Kliachko, T.R. Brueva, V.D. Nissenbaum, H.G. Karge, *Kinet. Katal.* 34 (5) (1993) 929.
- [26] L. Forni, F.P. Vatti, E. Ortoleva, *Zeolites* 12 (1992) 101.
- [27] D.B. Akolekar, V.R. Choudhary, *J. Catal.* 105 (1987) 416.